Inorganic Chemistry

ARTICLE

pubs.acs.org/IC

Lanthanide Nitrate Complexes of Tri-Isobutylphosphine Oxide: Solid State and CD_2Cl_2 Solution Structures

Allen Bowden,[†] Peter N. Horton,[‡] and Andrew W. G. Platt*[,§]

[†]Department of Chemistry and Analytical Sciences, The Open University, Walton Hall, Milton Keynes MK7 6BT, U.K.

[‡]School of Chemistry, University of Southampton, Highfield, Southampton SO17 1BJ, U.K.

[§]Faculty of Sciences, Staffordshire University, College Road, Stoke-on-Trent, ST4 2DE, U.K.

Supporting Information

ABSTRACT: The complexes $Ln(NO_3)_3L_3$ between $Ln(NO_3)_3$ and $^iBu_3PO$ (=L) have been prepared for Ln = La−Lu (excluding *Pm*). The isolated complexes have been characterized by infrared spectroscopy, mass spectrometry, and elemental analysis. The single crystal X-ray structures have been determined for representative complexes across the series Ln = Ce, Pr, Nd, Sm, Gd, Dy, Ho, Er, Tm, and Yb and show the coordination geometry around the metal to be the same with 9-coordinate lanthanide ions and bidentate nitrates. Subtle changes in the coordination of the nitrate ligand occur from Sm onward. Changes in the infrared spectra correlate well with changes in the X-ray structures. Solution properties have been examined by variable temperature multinuclear (^1H, ^{13}C, ^{15}N, and ^{31}P) NMR spectroscopy in CD_2Cl_2. The spectra of complexes of the early lanthanides are consistent with the presence of a single species in solution while those of the heavier lanthanides show that more than one complex is present in solution and that two inequivalent phosphorus environments are observable at low temperature. The fluxional behavior is lanthanide dependent with smaller ions giving static structures at higher temperature. Complexes with tricyclohexylphosphine oxide show that the dynamic NMR behavior is also related to the size of the ligand. Analysis of the lanthanide induced shifts indicates minor changes in solution structure occur from Sm onward which correlate well with the solid state structures.

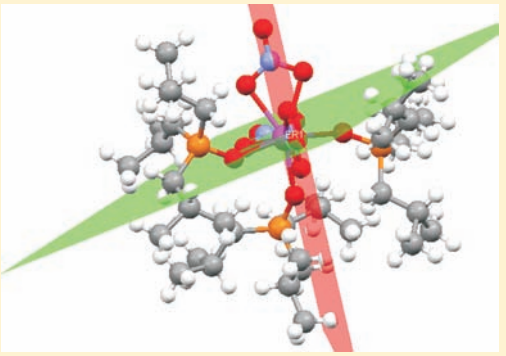

INTRODUCTION

The coordination chemistry of lanthanide nitrates with phosphine oxides has been studied extensively[1,2] because of the potential application of such complexes to nuclear reprocessing.[3,4] The relative ease with which their secondary structure can be altered to enhance solvent extraction properties and their chemically robust nature facilitates application in chemically aggressive environments. The complexes $Y(NO_3)_3(Ph_3PO)_3$ and $Y(NO_3)_3(Ph_2MePO)_3$ have a pseudo *mer*-octahedral geometry (if the nitrates are considered as occupying a single coordination site) but a *fac* arrangement with a less sterically demanding ligand in $Y(NO_3)_3(Me_3PO)_3$.[5] Complexes of lanthanides with Ph_2MePO give $Ln(NO_3)_3(Ph_2MePO)_3$ for all Ln with the lanthanum complex displaying a pseudo *fac*-octahedral geometry.[6] The structures of complexes with triphenylphosphine oxide have been investigated in some detail[7−9] and complexes of the type $Ln(NO_3)_3(Ph_3PO)_n$ where $n = 2$,[7] $n = 3$ and 4[8] can be isolated depending on reaction conditions. Structurally characterized complexes in the tetrakis(triphenylphosphine oxide) series show that for the lighter lanthanides two nitrates are chelating while one is monodentate and that as the ionic radii of the lanthanide decreases the monodentate nitrate is expelled from the primary coordination sphere giving the cationic complexes, $[Lu(NO_3)_2(Ph_3PO)_4]^+NO_3^-$.[8] The more bulky Cy_3PO forms a series of complexes with the core structure, $Ln(NO_3)_3(Cy_3PO)_3$ regardless of the proportions of metal to ligand used in the preparation,[10] with no 4:1 complexes being isolated, and one nitrate adopting a monodentate bonding mode for the later lanthanides.

While there seem to be no data on cone angles for phosphine oxides it seems reasonable that, to a first approximation, their steric demands would follow the order of those of the parent phosphines.[11] The fact that no 4:1 complexes can be prepared with Cy_3PO can be rationalized on steric grounds and ligands such as $^iBu_3PO$ which have similar steric demands to Ph_3PO might be expected to yield similar complexes.

We report here a detailed examination of the solid state and solution properties of complexes between lanthanide nitrates and $^iBu_3PO$.

SYNTHESIS

The reaction of $^iBu_3PO$ (L) with lanthanide nitrates in hot ethanol led to the formation of complexes which could be

Received: November 30, 2010
Published: February 20, 2011

isolated on prolonged cooling of the solutions at −20 °C for Ln = La to Tb. For the heavier lanthanides Dy to Lu, no crystallization occurred under these conditions, and the addition of diethylether followed by cooling was necessary. Elemental analysis shows that the isolated complexes all have the same composition $Ln(NO_3)_3L_3$. The crystals of the complexes of the heavier metals rapidly become opaque on standing which implies that these may have retained a small amount of solvent in the crystals, although these were not detected in X-ray analysis.

In all cases a further crop of the compounds could be obtained by evaporation of the filtrate to dryness followed by trituration with diethylether in which any excess ligand is soluble. Filtration gave solids with identical infrared spectra to the authentic samples. The characterizing data are given in the Experimental Section.

It is worth noting that in contrast to the Ph_3PO systems, and despite the fact that the ligands have similar steric properties, no complexes with more than three ligands bonded to the lanthanide could be isolated or detected in solution (see below).

SOLID STATE STRUCTURES

The structures of the complexes for Ln = Ce, Pr, Nd, Sm, Gd, Dy, Ho, Er, Tm, and Yb have been determined. The structures split into two main groups, the first three (Ce, Pr, and Nd) all exist in the space group $P2_12_12_1$ and have disorder with one of the phosphine oxide ligands. The other 7 (Gd, Sm, Er, Ho, Dy, Tm, and Yb) all lie in one form of the two chiral space groups $P4_12_12$ or $P4_32_12$ and have disorder with two of the phosphine oxide ligands (which are always the ligands which are ordered in the first group). Thus all the crystal structures exist in noncentrosymmetric space groups. In each case when crystallizing only one (or predominately one) form is present in the crystal studied. Unless many more crystal structures are tested for each compound, it is not possible to determine whether an equal amount of each form exists or not.

It is interesting to note that the crystals were sensitive to removal from the solvent, yet no significant solvent could be located in the crystal structures.

The complexes all have the same molecular connectivity and are 9-coordinate with three phosphoryl oxygen atoms and three bidentate nitrate ligands making up the primary coordination sphere. Details of the data collection and refinement for the crystal structures are given in Table 1, and selected bond lengths in Table 2. The structure of the Nd complex is shown in Figure 1 as a representative example. The geometry can be considered as a somewhat distorted *mer*-octahedron if the nitrate ions are considered as pseudo-monodentate ligands. These structures are similar to those of the lighter lanthanide complexes of bulkier Cy_3PO[10] and $La(NO_3)_3[Ph_2MePO]_3$.[6]

The Ln−O(N) distances decrease from 2.603 Å (Ce) to 2.439 Å (Yb) as might be expected from the lanthanide contraction. This trend was further examined by subtracting the 9-coordinate ionic radius of the lanthanide ion[12] from the observed Ln−O(N) distances, the result giving a distance adjusted for the effect expected from the lanthanide contraction. If the lanthanide contraction were the only factor responsible for the observed decrease these distances should be approximately constant. This was tested by a single factor ANOVA test over the data for all the complexes, and it was found that there was no significant difference, at a 95% confidence level, between the adjusted Ln−O(N) bond distances which average at 1.26 ± 0.01 Å. It thus seems that the observed decrease as the lanthanide series is traversed can be safely ascribed to the lanthanide contraction. On the basis of the idealized *mer*-octahedral geometry, we would expect the nitrate ligands to fall into two categories, the mutually "*trans*" nitrates and those "*trans*" to phosphine oxide. However, the Ln−O(N) distances are significantly different for each nitrate (paired *t* tests assuming unequal variance) with average Ln−O distances of 1.252(9), 1.263(10), and 1.277(8) Å corresponding to the two mutually "*trans*" nitrates and one "*trans*" to phosphine oxide, respectively. The longer average Ln−O(N) distances are associated with the nitrate ligand being less symmetrically bound to the metal with an average difference in Ln−O(N) of 0.075 Å for the nitrate "*trans*" to OP compared to 0.041 Å.

Significant differences occur in the angles around the nitrate ligands. The "cis" and "trans" N−Ln−N angles fall into two groups, Ce−Nd and Sm−Yb. Thus, while the "trans" angles are essentially the same 172.8 ± 0.5° (Ce−Nd) and 172.9 ± 0.3° (Sm−Yb) the two "cis" angles show significant differences; 99.6 ± 0.2° and 87.3 ± 0.1° for Ce−Nd compared with 94.9 ± 0.8° and 83.2 ± 1.2° for Sm−Yb. Similarly the dihedral angles between the O_2N planes of the "trans" nitrates follow the same pattern with a large drop in value between Nd and Sm. Thus for Ce−Nd the average angle is 88.3 ± 0.6° while for Sm−Yb this decreases to 77.7 ± 0.8°, a difference which is significant above a 99.99% confidence level. There are no similar significant differences between the internal O−N−O angles of the nitrate ligands. This decrease in the dihedral angle has the effect of reducing the steric interactions between the peripheral structure of the ligands. This can be seen in Figure 2 which shows as examples the Pr and Er complexes and the position of the ligands with respect to the O_2N planes. For the Pr complex the majority of the ligands structure is located in two of the four sectors defined by the intersection of the planes. The reduction of ionic radii will increase steric repulsions between the ligands, and from Sm onward each of the ligands is primarily located in a separate sector with the fourth being essentially unoccupied. The twisting of the nitrate ligands relative to one another will bring some increase in the electrostatic repulsions between the oxygen atoms, and this presumably is compensated for by the reduced ligand−ligand repulsions.

There are no significant differences within the Ln−O(P) distances either comparing the lengths as a function of the lanthanide or as a function of the "*cis*" or "*trans*" position within the complexes.

The infrared spectra are typical of those of lanthanide nitrate complexes of coordinated phosphine oxides.[10,13] The nitrate bands occur as a broad absorption at around 1440−1490 cm^{-1} assigned as ν_5, a sharper band due to ν_1 at 1300−1310 cm^{-1}, and a sharp, medium intensity peak from ν_2 at 1030−1035 cm^{-1}. The appearance of the ν_1 and ν_2 both show a weak trend of increasing wavenumber with the atomic number of the lanthanide, but their general appearance remains similar throughout. The position of ν_5, however, does change significantly as the lanthanide series is traversed. This band always shows a number of lower intensity features to higher wavenumber of the absorption maximum often with resolved fine structure apparent. This is possibly due to the presence of crystallographically different nitrates in the complex. The absorption becomes notably broader from Sm onward indicating that significant change in nitrate coordination occurs in this region. For the Lu complex ν_5 is resolved into two major peaks at 1466 and 1491 cm^{-1}. This change in appearance of ν_5 correlates well with the abrupt changes in bond angles at Sm discussed above. The infrared spectra of the La, Sm, and Lu complexes are shown in Figure 3. Samples enriched in ^{15}N (98%) have been prepared for the La

dx.doi.org/10.1021/ic102385p |*Inorg. Chem.* 2011, 50, 2553–2561

Table 1. Data Collection and Refinement for $Ln(NO_3)_3(^iBu_3PO)_3$

empirical formula	$C_{36}H_{81}CeN_3O_{12}P_3$	$C_{36}H_{81}N_3O_{12}P_3Pr$	$C_{36}H_{81}N_3NdO_{12}P_3$	$C_{36}H_{81}N_3O_{12}P_3Sm$	$C_{36}H_{81}GdN_3O_{12}P_3$	$C_{36}H_{81}DyN_3O_{12}P_3$	$C_{36}H_{81}HoN_3O_{12}P_3$	$C_{36}H_{81}ErN_3O_{12}P_3$	$C_{36}H_{81}N_3O_{12}P_3Tm$	$C_{36}H_{81}N_3O_{12}P_3Yb$
formula weight	981.07	981.86	985.19	991.3	998.2	1003.45	1005.88	1008.21	1009.88	1013.99
temperature	120(2) K	120(2) K	120(2) K	120(2) K	120(2) K	120(2) K	120(2) K	120(2) K	120(2) K	120(2) K
wavelength	0.71073 Å	0.71073 Å	0.71073 Å	0.71073 Å	0.71073 Å	0.71073 Å	0.71073 Å	0.71073 Å	0.71073 Å	0.71073 Å
crystal system	orthorhombic	orthorhombic	orthorhombic	tetragonal	tetragonal	tetragonal	tetragonal	tetragonal	tetragonal	tetragonal
space group	$P2_12_12_1$	$P2_12_12_1$	$P2_12_12_1$	$P4_12_12$	$P4_12_12$	$P4_32_12$	$P4_12_12$	$P4_12_12$	$P4_32_12$	$P4_32_12$
unit cell dimension										
a, Å	14.3658(7)	14.3481(9)	14.3298(5)	15.2470(5)	15.2683(4)	15.3937(10)	15.2959(6)	15.3066(7)	15.2872(6)	15.3887(6)
b, Å	14.5103(7)	14.4845(9)	14.4760(5)	15.2470(5)	15.2683(4)	15.3937(10)	15.2959(6)	15.3066(7)	15.2872(6)	15.3887(6)
c, Å	23.9483(8)	23.9651(15)	23.9774(9)	43.4821(18)	43.3340(16)	43.421(4)	43.217(2)	43.170(3)	43.078(3)	43.295(3)
volume Å^3	4992.1(4)	4980.5(5)	4973.8(3)	10108.3(6)	10102.1(5)	10289.2(13)	10111.3(7)	10114.3(9)	10067.4(8)	10252.7(8)
Z	4	4	4	8	8	8	8	8	8	8
density (calculated) Mg/m^3	1.305	1.309	1.316	1.303	1.313	1.296	1.322	1.324	1.333	1.314
absorption coefficient mm^{-1}	1.061	1.128	1.194	1.309	1.461	1.597	1.712	1.807	1.911 [1]	1.970
F(000)	2068	2072	2076	4168	4184	4200	4208	4216	4224	4232
crystal	cut block; colorless	cut block; colorless	cut block; pale purple	cut block; colorless	block; colorless	plate; colorless	block; colorless	block; pale pink	cut block; colorless	cut block; colorless
crystal size mm^3	0.18 × 0.16 × 0.07	0.66 × 0.47 × 0.28	0.26 × 0.13 × 0.08	0.16 × 0.13 × 0.10	0.32 × 0.24 × 0.18	0.90 × 0.66 × 0.12	0.22 × 0.15 × 0.12	0.46 × 0.34 × 0.30	0.26 × 0.18 × 0.08	0.30 × 0.24 × 0.12
θ range for data collection	2.91−27.48°	2.94−27.48°	2.91−27.48°	2.99−27.48°	2.98−27.48°	2.96−25.00°	2.98−27.48°	2.98−25.00°	3.02−27.48°	2.96−24.99°
index ranges	$-18 \le h \le 18$, $-18 \le k \le 18$ $-31 \le l \le 31$	$-16 \le h \le 18$ $-10 \le k \le 18$ $-31 \le l \le 17$	$-18 \le h \le 18$ $-18 \le k \le 18$ $-30 \le l \le 31$	$-17 \le h \le 18$ $-19 \le k \le 19$ $-56 \le l \le 56$	$-19 \le h \le 19$ $-19 \le k \le 19$ $-56 \le l \le 56$	$-18 \le h \le 18$ $-18 \le k \le 18$ $-42 \le l \le 51$	$-19 \le h \le 19$ $-19 \le k \le 19$ $-56 \le l \le 51$	$-18 \le h \le 17$ $-18 \le k \le 15$ $-49 \le l \le 51$	$-19 \le h \le 19$ $-17 \le k \le 19$, $-55 \le l \le 55$	$-18 \le h \le 18$ $-18 \le k \le 18$ $-51 \le l \le 51$
reflections collected	34717	24066	31534	97636	62553	35049	51946	59748	46743	38179
independent reflections	11396 [R_{int} = 0.0706]	11189 [R_{int} = 0.0406]	11004 [R_{int} = 0.0504]	11524 [R_{int} = 0.0955]	11383 [R_{int} = 0.0620]	8880 [R_{int} = 0.0833]	11537 [R_{int} = 0.0682]	8906 [R_{int} = 0.1594]	10881 [R_{int} = 0.0661]	8677 [R_{int} = 0.0687]
completeness to θ = 27.48°	99.70%	99.50%	98.40%	99.70%	99.50%	98.70%	99.60%	99.70%	96.90%	98.30%
absorption correction	semi-empirical from equivalents	semi-empirical from equivalents	semi-empirical from equivalents	semi-empirical from equivalents	semi-empirical from equivalents	semi-empirical from equivalents	semi-empirical from equivalents	semi-empirical from equivalents	semi-empirical from equivalents	semi-empirical from equivalents
max. and min transmission	0.9294 and 0.8320	0.7430 and 0.5231	0.9105 and 0.7466	0.8802 and 0.8179	0.7790 and 0.6522	0.8314 and 0.3274	0.8209 and 0.7045	0.6132 and 0.4903	0.8622 and 0.6364	0.7980 and 0.5895
refinement method	full-matrix least-squares on F^2	full-matrix least-squares on F^2	full-matrix least-squares on F^2	full-matrix least-squares on F^2	full-matrix least-squares on F^2	full-matrix least-squares on F^2	full-matrix least-squares on F^2	full-matrix least-squares on F^2	full-matrix least-squares on F^2	full-matrix least-squares on F^2
data/restraints/parameters	11396/504/641	11189/492/636	11004/378/624	11524/970/745	11383/976/750	8880/976/751	11537/946/751	8906/982/750	10881/964/750	8677/1274/745
goodness-of-fit on F^2	1.197	1.28	1.1	1.048	1.072	1.048	1.048	1.042	1.036	1.176
final *R* indices [$F^2 > 2\sigma(F^2)$]	*R1* = 0.0830	*R1* = 0.0781	*R1* = 0.0789	*R1* = 0.0823	*R1* = 0.0516	*R1* = 0.0801	*R1* = 0.0588	*R1* = 0.0637	*R1* = 0.0566	*R1* = 0.1039
	wR2 = 0.1465	*wR2* = 0.1908	*wR2* = 0.1834	*wR2* = 0.1537	*wR2* = 0.1058	*wR2* = 0.2233	*wR2* = 0.1385	*wR2* = 0.1138	*wR2* = 0.1166	*wR2* = 0.2051
R indices (all data)	*R1* = 0.1026	*R1* = 0.0789	*R1* = 0.0798	*R1* = 0.1415	*R1* = 0.0900	*R1* = 0.1082	*R1* = 0.0857	*R1* = 0.1423	*R1* = 0.1027	*R1* = 0.1339
	wR2 = 0.1528	*wR2* = 0.1911	*wR2* = 0.1839	*wR2* = 0.1777	*wR2* = 0.1208	*wR2* = 0.2577	*wR2* = 0.1538	*wR2* = 0.1370	*wR2* = 0.1380	*wR2* = 0.2182
absolute structure parameter	0.04(2)	0.14(2)	0.10(2)	0.07(3)	0.035(14)	0.16(3)	0.097(16)	0.049(16)	0.089(15)	0.13(3)
largest diff. peak and hole	1.563 and −2.528 e Å^{-3}	1.570 and −3.606 e Å^{-3}	1.793 and −2.299 e Å^{-3}	1.879 and −1.987 e Å^{-3}	0.812 and −1.645 e Å^{-3}	1.449 and −1.907 e Å^{-3}	0.972 and −1.912 e Å^{-3}	0.616 and −0.598 e Å^{-3}	0.757 and −1.620 e Å^{-3}	1.334 and −1.751 e Å^{-3}

dx.doi.org/10.1021/ic102385p |*Inorg. Chem.* 2011, 50, 2553–2561

Table 2. Selected Bond Distances (Å) in $Ln(NO_3)_3(^iBu_3PO)_3$

	Ce	Pr	Nd	Sm	Gd	Dy	Ho	Er	Tm	Yb
Ln−O1	2.371(6)	2.393(6)	2.358(5)	2.15(2)	2.4029(15)	2.17(2)	2.174(19)	2.23(2)	2.30(2)	2.216(16)
Ln−O2	2.402(5)	2.340(6)	2.378(6)	2.194(12)	2.196(16)	2.325(19)	2.137(19)	2.16(2)	2.13(2)	2.29(2)
Ln−O3	2.353(13)	2.364(11)	2.422(18)	2.359(5)	2.326(3)	2.293(8)	2.290(4)	2.283(5)	2.267(4)	2.264(9)
Ln−O11	2.607(6)	2.587(8)	2.592(7)	2.501(7)	2.558(4)	2.550(10)	2.441(5)	2.434(6)	2.528(5)	2.525(11)
Ln−O12	2.623(6)	2.606(7)	2.556(8)	2.572(7)	2.484(4)	2.451(9)	2.535(5)	2.529(6)	2.411(5)	2.403(10)
Ln−O21	2.602(6)	2.591(7)	2.583(7)	2.517(7)	2.512(4)	2.462(10)	2.500(5)	2.499(6)	2.408(5)	2.396(11)
Ln−O22	2.623(6)	2.600(7)	2.564(7)	2.508(8)	2.490(5)	2.484(9)	2.332(5)	2.421(6)	2.494(6)	2.490(11)
Ln−O31	2.565(6)	2.595(7)	2.560(7)	2.505(7)	2.475(4)	2.496(9)	2.480(5)	2.475(6)	2.407(6)	2.352(12)
Ln−O32	2.599(6)	2.565(8)	2.558(7)	2.557(7)	2.546(5)	2.458(9)	2.431(6)	2.418(7)	2.253(5)	2.466(11)

Table 3. ^{31}P NMR Data for $Ln(NO_3)_3(^iBu_3PO)_3$ in CD_2Cl_2

temperature /°C		La	Ce	Pr	Nd	Sm	Eu	Tb	Dy	Ho	Er	Tm	Yb	Lu
20	major species	58.1	91.2	136.1	131.1	57.7	−52.3	−66.8	67.9	−10.7	−113.6	−80.9	12.2	60.6 P_a 61.5 P_b
	minor species							−123.4	−49.0	−52.6	−59.0	−20.01	43.5	
−90	major species	59.3	117.2	234.9	200.6	67.4	−109.2 P_a −55.4 P_b	−317.8	180.7	473.4	−284.4 P_a −170.2 P_b	−358.8 P_a −57.8 P_b	−116.9 P_a 67.6 P_b	60.8 P_a 62.6 P_b
	minor species		114.3			66.0					−80.5	−76.8	30.0	62.7 P_a 63.6 P_b
	minor species												4.9	63.5

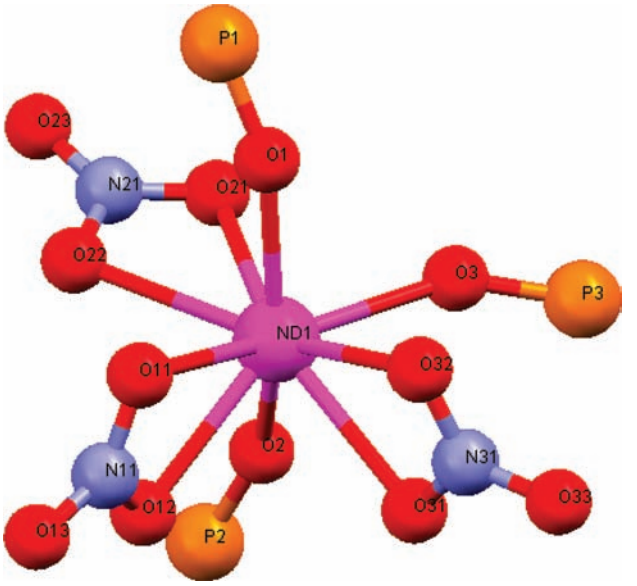

Figure 1. Core structure of the $Nd(NO_3)_3(^iBu_3PO)_3$. Carbon and hydrogen atoms have been omitted for clarity.

and Lu complexes and show significant decreases in the wavenumber of absorption maxima for all bands confirming these assignments. The ν_{PO} stretch is seen as an intense band split into two at 1117 and 1097 cm^{-1} again reflecting the inequivalent environment of the ligands in the complex. The position of this absorption is at lower wavenumber than that of the free ligand (for which ν_{PO} = 1155 cm^{-1}) and shows no dependence on the lanthanide ion. In view of the similarity of the P−O distances between the complexes across the series this is not surprising. We have reported a similar effect in the complexes of $[LnBr_2(Ph_3PO)_4]Br$ previously.[14]

SOLUTION PROPERTIES

All the complexes are readily soluble in dichloromethane. Although this is not an ideal solvent for conductivity studies[15] it does have some merit in that it is generally non coordinating and thus unlikely to promote ionization of dissolved complexes. Conductivity measurements indicate that although the complexes are essentially non conducting there is a small but significant rise in the molar conductance from about 1×10^{-5} Sm^2 mol^{-1} (La−Sm) to about 5×10^{-5} Sm^2 mol^{-1} (Eu−Lu). Although these values are very much smaller than those observed for 1:1 electrolytes, for which values in the region of 0.005 Sm^2 mol^{-1} are typically obtained,[6] they do indicate that dissociation of nitrate ion occurs to a small extent in solution. That this occurs for the heavier lanthanides is consistent with loss of nitrate in solution as a result of the lanthanide contraction.

The solution NMR spectra (^1H, ^{13}C, ^{31}P, and some ^{15}N), were recorded between 20 °C to −90 °C in CD_2Cl_2 using approximately 0.025 M solutions. The complexes are stable in solution, and the spectra do not change on standing over 4 months. The phosphorus spectra, in particular, are informative in elucidation of the solution behavior. The results for these spectra at 20 °C and −90 °C are shown in Table 3. The paramagnetic complexes show the expected strong temperature dependence of the chemical shift.[16] The spectra at 20 °C show one peak for La−Eu indicating the presence of a single species in solution or rapid exchange between two or more environments. For the heavier metals there is a major peak accounting for 90−97% of the integrated signal area, together with a lower intensity resonance assigned to the presence of other complexes present in low concentration in solution. This could either be a different isomer (for instance the pseudo *fac*-isomer), or be due to dissociation of nitrate or L which might occur to reduce the steric strain particularly in the complexes of the heavier metals.

dx.doi.org/10.1021/ic102385p |*Inorg. Chem.* 2011, 50, 2553–2561

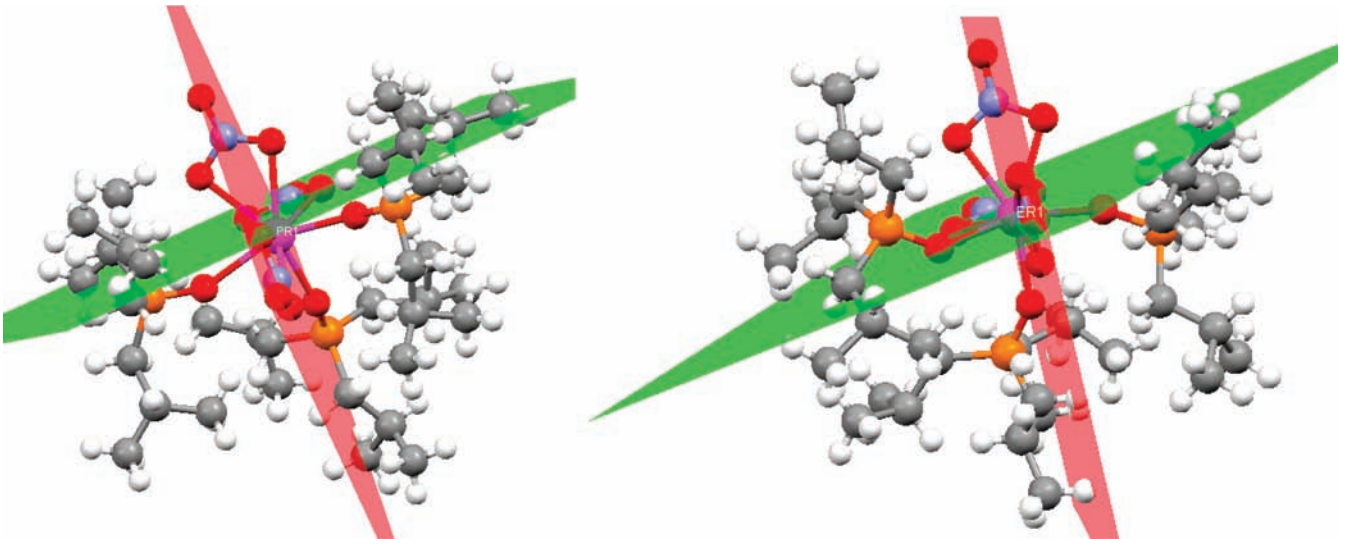

Figure 2. Structure of the Pr and Er complexes showing the variation in ligand occupancy as the ionic radius decreases.

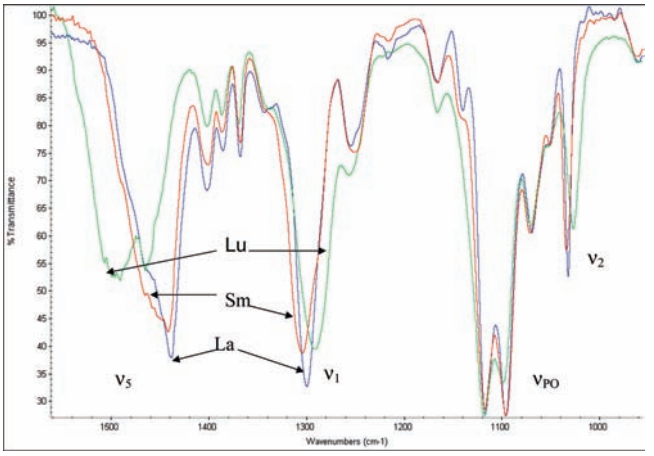

Figure 3. Infrared spectra of $Ln(NO_3)_3(^iBu_3PO)_3$ Ln = La, Sm, Lu.

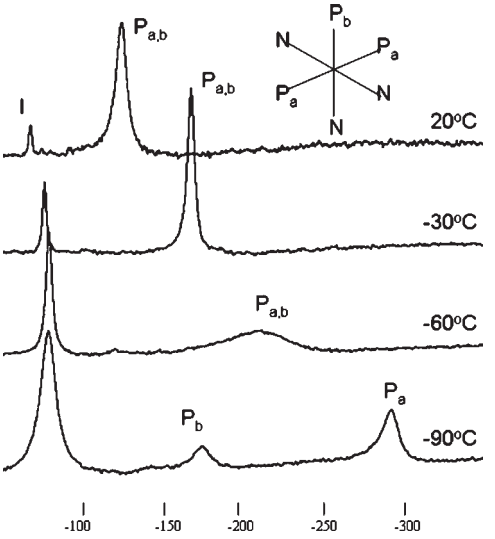

Figure 4. Variable temperature ^{31}P NMR spectra for $Er(NO_3)_3$-$(^iBu_3PO)_3$ in CD_2Cl_2 I = different complex in solution.

The marginal increase in conductivity for the complexes of the heavier lanthanides is consistent with ionization occurring to a small extent. The ^{15}N NMR spectra, however, show no evidence for the presence of free nitrate in solution, but from the very low values of conductivity we would expect any signal to be of low intensity and probably not observable. There is no evidence of dissociation of L as no signal was observed in the spectra of any of the complexes in the region 47 ppm even at −90 °C, which would indicate its presence.

The energy difference between different geometries for high coordination number complexes is generally thought to be small. Thus in addition to the geometries observed in the solid state, lanthanide complexes are likely to have available other structures at room temperature. The rapid interchange between such alternative geometries may explain the simple spectra observed for many lanthanide complexes. The observation of intramolecular exchange between two inequivalent sites in the same molecule is rare for lanthanide complexes even where crystal structures suggest that these are present. In some cases static structures can be observed by NMR spectroscopy. Examples have been recently observed in macrocyclic complexes.[17,18] Similarly the exchange between "free" and coordinated PO groups in a europium complex with a tetradentate calix-4-arene is rapid at 60 °C while a static structure is observed at −70 °C.[19] The pseudo *mer*-octahedral complexes of Ph_3PO[8] and Ph_2MePO[6] do not show the presence of static structures on the NMR time scale at −50 and 0 °C respectively. In the present study decreasing the temperature the complexes of the lighter lanthanides (La−Sm) causes a considerable increase in the line width which could imply that fluxional behavior is occurring. For these complexes the temperature cannot be lowered sufficiently to observe NMR spectra associated with a static structure. However, the signals from other complexes also broaden and by −90 °C split into two separate signals with an approximately 2:1 intensity ratio. This was observed for the Eu and Er−Lu complexes, but not for Tb, Dy, and Ho, possibly because of very large linewidths for these complexes, or accidental coincidence of chemical shifts. We would expect here that integrated peak area would give a good measure of the populations of these environments because of the enhanced relaxation rates of nuclei in the vicinity of paramagnetic

dx.doi.org/10.1021/ic102385p |*Inorg. Chem.* 2011, 50, 2553–2561

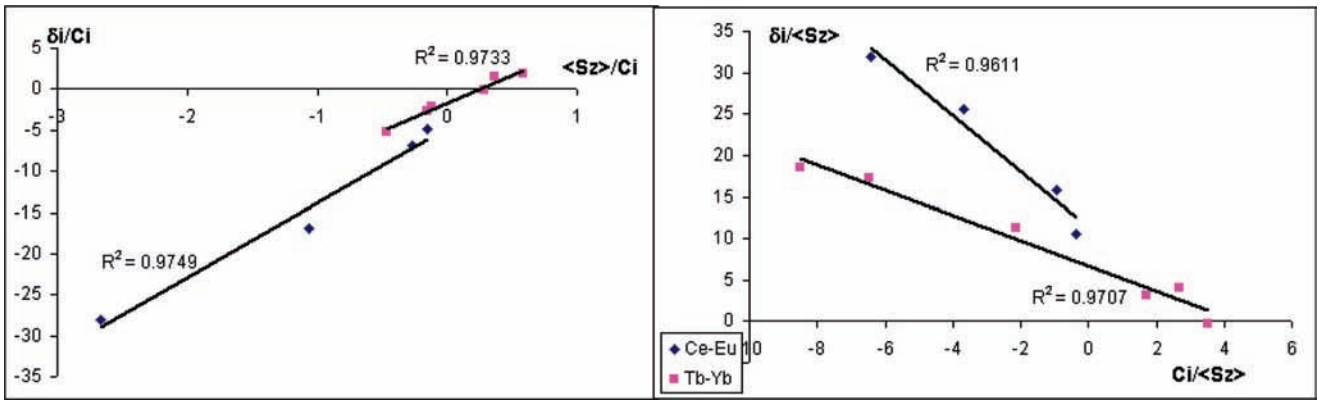

Figure 5. Single nucleus LIS plots at 17 °C.

ions. It thus seems reasonable to attribute these observations to the presence of rigid structures at −90 °C similar to those observed in the solid state. The ^{31}P NMR spectra of the Er complex is shown as a representative example in Figure 4. Although we have not carried out a detailed study, we note that this variable temperature behavior is lanthanide dependent. Thus two well resolved signals can be seen for the Lu complex at −30 °C while the Er complex has to be cooled to −90 °C to observe the same effect. For all the complexes of the heavier lanthanides the spectra show additional peaks due to other complexes in solution. In the case of Lu at −90 °C this peak is also split into two peaks at 63.6 and 62.7 ppm in approximately 1:2 ratio. This implies that a complex similar in structure to the major species is present in which two phosphorus atoms are in a chemically identical or similar environment but different from the third. No $^4J_{PP}$ is observed for the Lu complex, and its value must be lower than 30 Hz, the line width for the complex at this temperature. The ^{15}N NMR spectra obtained over the same temperature range for the La and Lu complexes give findings in agreement with the above. Thus the La complex shows a single resonance at all temperatures between 138.91−139.11 ppm (relative to $NaNO_3$) while the Lu complex shows a single peak at 136.16 ppm at 20 °C and two clearly resolved signals at 136.85 and 136.70 ppm in an approximately 1:2 ratio at −90 °C due to the two inequivalent sets of nitrate ligands in the complex. The mechanism of fluxionality in these complexes does not appear to involve dissociation of either ^{i}Bu$_3$PO or NO_3^- followed by rearrangement. Presumably this requires the formation of another nine coordinate geometry of similar energy to the solid state structures, possibly the pseudo *fac*-octahedral isomer, or the transient formation of a monodentate nitrate followed by reorganization as postulated for complexes of 4,4,4-trifluoro-1-(2-thienyl)-1,3-butanedione.[20] That this is at higher energy for the smaller lanthanides is probably a result of increased steric interactions between the ^{i}Bu groups. To test whether the size of the peripheral structure of the ligand influences the rigidity of the complexes we examined the ^{31}P NMR spectra of Ln$(NO_3)_3$-$(Cy_3PO)_3$ (Ln = La, Nd, Eu, and Tm)[10] where the bulkier tricyclohexylphosphine oxide ligand might be expected to show a significant effect. The La, Nd, and Eu complexes all show a single peak in their spectra between 20 °C and −30 °C, and for the La complex no further change occurs on cooling to −90 °C with a shift range of 59.9−60.5 ppm. In contrast at −60 °C, the Nd and Eu complexes each show two peaks in a 1:2 ratio at 177 and 254 ppm and −106.4 and −131.9 ppm, respectively. The linewidths for the Nd complex are considerably greater at ∼4800 Hz, but sharper on cooling to −90 °C indicating that, in part, the linewidths are due to exchange broadening at −60 °C. The Tm complex shows spectra consistent with a static structure at 20 °C. In contrast to the behavior of the Cy_3PO described above a static structure cannot be observed for the Nd complex while a temperature of −90 °C required for Eu$(NO_3)_3$(^{i}Bu$_3$PO)$_3$.

The differences in behavior of complexes of ^{i}Bu$_3$PO compared with those of Ph_3PO where static structures are not observed for any of the lanthanide ions, is difficult to explain on steric grounds alone since the parent phosphines have very similar cone angles.[11] In this case it is likely that ^{i}Bu$_3$PO is a better donor to lanthanide ions than Ph_3PO. This would imply a stronger interaction between ligand and lanthanide ion which may increase the barrier to fluxional behavior.

Many lanthanide complexes are labile in solution, and to examine any intermolecular exchange processes spectra were obtained in the presence of a small quantity of free ligand. For the La complex the room temperature spectrum showed a single broadened resonance ($\Delta\nu_{1/2}$ = 14 Hz in the absence of ligand compared to $\Delta\nu_{1/2}$ = 212 Hz in the presence of free ligand) indicative of rapid ligand exchange on the NMR time scale between free and coordinated environments. At −90 °C this exchange is slow on the NMR time scale and two signals are observed at 59.3 ppm ($\Delta\nu_{1/2}$ = 6 Hz) assigned to the complex and 47.6 ppm assigned to free ligand. For the Lu complex the exchange is slower at room temperature with two broad peaks resolved at 61.5 ppm $\Delta\nu_{1/2}$ = 490 Hz (compared with 31 Hz in the absence of free ligand) and 47.1 ppm due to the free ligand. At −90 °C separate sharp signals are observed for all Lu containing species and free ligand.

The ^{1}H and ^{13}C NMR spectra are as expected for the coordinated ligand, with readily assignable spectra for Ln = La−Eu, Lu. Here the paramagnetic shifts decrease with an increase in separation of the observed nucleus from the paramagnetic ion. Thus for ^{13}C the change on chemical shifts are $\Delta\delta$ (CH_2) ∼ 6 ppm, $\Delta\delta$ (CH) ∼ 4 ppm, and $\Delta\delta$ (CH3) ∼ 2 ppm with the largest shifts observed for the Pr complex. A similar effect is observed in the ^{1}H spectra. The full data are presented in the Supporting Information. The spectra of the complexes of the heavier metals, Ln = Tb−Yb are not fully interpretable often showing broad unresolved signals at all temperatures.

Analysis of lanthanide induced shifts has previously been used to deduce whether structures remain constant across the lanthanide series in solution. Analyses based on the observation of one, two, and three nuclei[21,22] in a complex have been developed. The one nucleus method strictly applies only to axially symmetric complexes. In this method plots of δ_i/C_i versus $\langle S_z\rangle_i/C_i$ and

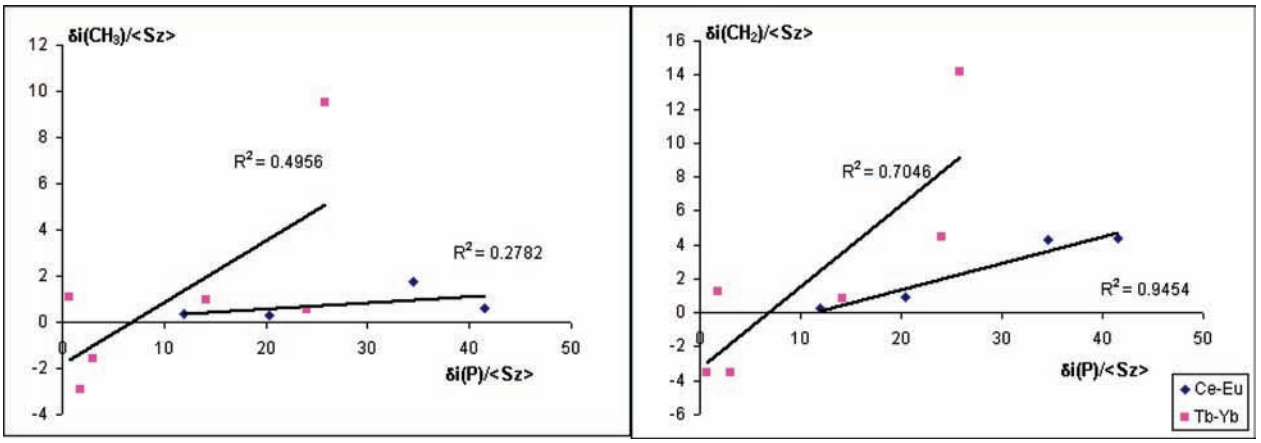

Figure 6. Two nucleus LIS plots at −30 °C.

$\delta_i/\langle S_z\rangle_i$ versus $C_i/\langle S_z\rangle_i$ are analyzed. δ_i is the paramagnetic shift for a given complex where $\delta_i = \delta_{Ln} - 1/2[\,\delta_{La} - \delta_{Lu}]$ and δ_{Ln}, δ_{La}, and δ_{Lu} are the observed shifts for the lanthanide complex and the lanthanum and lutetium complexes, respectively. $\langle S_z\rangle_i$ is the spin expectation value for a particular lanthanide ion and C_i is the Bleaney factor for the lanthanide ion which depends only on its electronic configuration. Both plots are expected to be linear if there is structural uniformity in solution across the series, while breaks in one or both imply minor or major structural changes respectively.[23] If two nuclei can be observed a plot of $\delta_i/\langle S_z\rangle_i$ versus $\delta_j/\langle S_z\rangle_j$ where δ_i and δ_j are the paramagnetic shifts of two different nuclei in the same complex, should be linear if there are no structural changes in solution. The three nucleus method is independent of the symmetry of the complex, but we have been unable to obtain reliable chemical shift data for ^{1}H and ^{13}C for all of the complexes. Analysis by the one nucleus method has been carried out on the data at room temperature and at −30 °C for the ^{31}P NMR data and indicates that there is a change in structure at the middle of the series.

Thus, plots of δ_i/C_i versus $\langle S_z\rangle_i/C_i$ and $\delta_i/\langle S_z\rangle_i$ versus $Ci/\langle S_z\rangle_i$ both show separate good linear trends for Ce−Eu and Tb−Yb as shown in Figure 5. The ^{13}C data afforded sufficient interpretable spectra to carry out a two nucleus plot of ^{13}C versus ^{31}P data at −30 °C. Thus, both the plots of $\delta_i(CH_3)/\langle S_z\rangle_i$ versus δ_i (P)$/\langle S_z\rangle_i$ and $\delta_i(CH_2)/\langle S_z\rangle_i$ versus δ_i (P)$/\langle S_z\rangle_i$ show two linear regions corresponding to Ce−Eu and Tb−Yb as shown in shown in Figure 6. It must be noted here, however, that the correlation coefficients for the linear plots are much less convincing than those obtained from the single nucleus plots. This may, in part arise from uncertainties in some of the assignments in the ^{13}C spectra as well as any inherent uncertainties due to deviations from the ideal symmetry required by the model and any changes in $\langle S_z\rangle_i$ with temperature. The analysis of the lanthanide induced shifts implies that minor changes in the solution structures occur in the region of samarium, a finding which correlates well with the change in the coordination of the nitrate ligand observed in the solid state structures and in the infrared spectra of the complexes.

CONCLUSION

Complete uniformity of structures for a series of complexes across the lanthanides is rare; for example, normally the decrease in ionic radii is accompanied by changes in the coordination of nitrate from η^2 to η^1 bonding, or ionization to reduce the steric strain. In these complexes there are no gross changes in structure as a result of the decrease in ionic radii, but a rather more subtle change in the coordination geometry of the nitrate ligands which allows a decrease in steric interaction between the peripheral structure of the ^{i}Bu$_3$PO ligands.

We have demonstrated that the solid state structures of the $Ln(NO_3)_3(^iBu_3PO)_3$ are similar in solution and that changes in both occur between the lighter and heavier metals probably because of the coordination of the nitrate ligands. The NMR spectra show the first examples of static structures for lanthanide nitrate complexes with simple monodentate ligands and that the dynamic behavior is lanthanide dependent and also related to the steric effect of the bulky ligand.

EXPERIMENTAL SECTION

Suitable crystals were selected and data collected on a Bruker Nonius KappaCCD Area Detector at the window of a Bruker Nonius FR591 rotating anode (Mo K_α = 0.71073 Å) driven by COLLECT[24] and DENZO[25] software at 120 K. The structures were determined in SHELXS-97[26] and refined using SHELXL-97.[27] All non-hydrogen atoms were refined anisotropically, with all hydrogen atoms placed geometrically using standard riding models.

In all the structures either one or two of the phosphine oxide ligands were disordered over 2 sites. In each case, these ligands had both thermal and geometrical restraints applied (SIMU and SAME commands in SHELX).

In some of the structures there are cavities of size suitable for small solvent molecules such as ethanol, but in each case when attempting to place atoms in the cavity, and allowing their occupancy to freely refine, they fell below 10% occupancy and still had poor displacement parameters resulting in no appreciable change in the R-factors. Thus, no solvent was included in the final modeling of the structures.

Crystallographic data (excluding structure factors) for the structures in this paper have been deposited with the Cambridge Crystallographic Data Centre as supplementary publication numbers 783613 to 783622. Copies of the data can be obtained, free of charge, on application to CCDC, 12 Union Road, Cambridge CB2 1EZ, U.K. (Fax: +44(0)-1223-336033 or e-mail: deposit@ccdc.cam.ac.uk

Mass spectra were obtained on a Thermofisher LTQ Orbitrap XL at the EPSRC National Mass Spectrometry Service Centre at Swansea University. Samples (~10 mg) were dissolved in 300 μL of CH_2Cl_2 and were loop injected into a stream of methanol.

Infrared spectra were recorded with a resolution of ±2 cm^{-1} on a Thermo Nicolet Avatar 370 FT-IR spectrometer operating in ATR mode. Samples were compressed onto the optical window and spectra recorded without further sample pretreatment.

Table 4. Characterizing Data for the Complexes

		elemental analysis % observed (required)			
complex	yield %	C	H	N	mass spectrometry[a] observed[b] (calculated)
$La(NO_3)_3L_3$	36	44.14 (44.13)	8.39 (8.13)	4.32 (4.18)	917.4208 (917.4213)
$Ce(NO_3)_3L_3$	72	44.10 (44.07)	8.72 (8.32)	4.20 (4.28)	918.4191 (918.4204)
$Pr(NO_3)_3L_3$	60	44.32 (44.04)	8.70 (8.31)	4.21 (4.28)	919.4231 (919.4226)
$Nd(NO_3)_3L_3$	62	43.33 (43.89)	8.57 (8.29)	4.12 (4.26)	922.4247 (922.4258)
$SmNO_3)_3L_3$	65	43.38 (43.62)	8.61 (8.24)	4.16 (4.24)	930.4342 (930.4348)
$Eu(NO_3)_3L_3$	92	43.04 (43.55)	8.08 (8.22)	4.29 (4.23)	931.4362 (931.4362)
$Gd(NO_3)_3L_3$	73	42.85 (43.32)	8.52 (8.16)	4.13 (4.20)	936.4392 (936.4400)
$Tb(NO_3)_3L_3$	65	42.91 (43.24)	8.10 (8.43)	4.34 (3.95)	937.4400 (937.4403)
$Dy(NO_3)_3L_3$	56	43.06 (43.09)	8.14 (8.14)	4.24 (4.19)	942.5 (942.4)[c]
$Ho(NO_3)_3L_3$	52	42.95 (42.99)	8.08 (8.12)	4.28 (4.18)	943.4461 (943.4453)
$Er(NO_3)_3L_3$	55	42.87 (42.89)	8.20 (8.10)	4.32 (4.17)	946.4484 (946.4477)
$Tm(NO_3)_3L_3$	65	42.76 (42.82)	8.19 (8.08)	4.24 (4.16)	947.4488 (947.4492)
$Yb(NO_3)_3L_3$	70	42.56 (42.64)	8.17 (8.05)	4.27 (4.14)	952.4541 (952.4545)
$Lu(NO_3)_3L_3$	76	42.33 (42.56)	7.92 (8.04)	3.80 (4.13)	953.4567 (953.4557)

[a] Electrospray ionization from CH_2Cl_2 solution. [b] m/z for the highest intensity peak in the profile of $[Ln\text{-}NO_3]^+$. [c] Spectrum obtained at low resolution.

NMR spectra were recorded on a JEOL EX 400 in CD_2Cl_2 solutions approximately 20 mg of complex dissolved in about 0.75 mL of solvent.

Conductivity measurements were made on 0.001 M solution of the complexes in dichloromethane using a Hanna HI 9033 multi range conductivity meter.

The complexes were prepared by two general methods depending on the lanthanide. For the lighter lanthanides ethanolic solutions of the ligand and the lanthanide nitrate were mixed and warmed briefly to boiling. The resulting solution was cooled to −20 °C. On prolonged standing crystals were deposited for Ln = La−Tb. For the heavier metals no crystals formed when treated as above. The addition of diethylether and standing at −20 °C for several days led to the formation of crystals for Ln = Dy−Lu.

Evaporation of the filtrates followed by trituration with diethylether led to the isolation of powders whose infrared spectra were identical to the crystals isolated above. The characterizing data are given in Table 4, and full details of individual preparations as Supporting Information.

■ ASSOCIATED CONTENT

Supporting Information. Further details are given on the synthesis of complexes and the NMR data, and crystallographic data in CIF format. This material is available free of charge via the Internet at http://pubs.acs.org.

■ AUTHOR INFORMATION

Corresponding Author
*E-mail: a.platt@staffs.ac.uk.

■ ACKNOWLEDGMENT

We are grateful to the EPSRC for the use of the National Mass Spectrometry Service at Swansea University and the Royal Society of Chemistry for support from their research fund.

■ REFERENCES

(1) Cotton, S. A. *Comprehensive Coordination Chemistry II*; McCleverty, J. A., Mayer, T. J., Eds.; Elsevier: Amsterdam, The Netherlands, 2004; Vol. 3, p 93.

(2) T. S.Lobana In *The Chemistry of Organophosphorus Compounds*; Hartley, F. R., Ed.; John Wiley and sons: New York, 1992; Vol. 2, p 409.

(3) Nash, K. L.; Lavallette, C.; Borkowski, M.; Paine, R. T.; Gan, X. *Inorg. Chem.* **2002**, *41*, 5849. Gan, X.; Rapko, B. M.; Duesler, E. N.; Paine, R. T. *Polyhedron* **2005**, *24*, 469.

(4) Turanov, A. N.; Karandashev, V. K.; Yarkevich, A. N.; Safronova, Z. V. *Solvent Extr. Ion Exch.* **2004**, *22*, 391.

(5) Deakin, L.; Levason, W.; Popham, M. C.; Reid, G.; Webster, M. *J. Chem. Soc., Dalton Trans.* **2000**, 2439.

(6) Bosson, M.; Levason, W.; Patel, T.; Popham, M. C.; Webster, M. *Polyhedron* **2001**, *20*, 2055.

(7) Levason, W.; Newman, E. H.; Webster, M. *Acta Crystallogr.* **2000**, *C56*, 1308.

(8) Levason, W.; Newman, E. H.; Webster, M. *Polyhedron* **2000**, *19*, 2697.

(9) Glazier, M. J.; Levason, W.; Matthews, M. L.; Thornton, P. L.; Webster, M. *Inorg. Chim. Acta* **2004**, *357*, 1083.

(10) Hunter, A. P.; Lees, A. M. J.; Platt, A. W. G. *Polyhedron* **2007**, *26*, 4865–4876.

(11) Tolman, C. A. *Chem. Rev.* **1977**, *77*, 345.

(12) Shannon, R. D. *Acta Crystallogr.* **1976**, *A32*, 751.

(13) Nakamoto, K. *Infrared and Raman spectra of Inorganic and Coordination compounds*, 5th ed.; J.Wiley and Sons: New York, 1997.

(14) Bowden, A., Platt, A. W. G., Singh, K., Townsend, R. *Inorg. Chim. Acta* **2010**, *363*, 243.

(15) Rosenthal, M. R.; Drago, R. *Inorg. Chem.* **1965**, *4*, 840.

(16) Zuo, C. S.; Metz, K. R.; Sun, Y.; Sherry, A. D. *J. Magn. Reson.* **1998**, *133*, 53.

(17) Regueiro-Figueroa, M.; Esteban-Gomez, D.; de Blas, A.; Rodrigues-Blas, T.; Platas-Ingesias, C. *Eur. J. Inorg. Chem.* **2010**, 3586.

(18) Purgel, M.; Baranyai, Z.; de Blas, A.; Rodrigues-Blas, T.; Banyai, I.; Platas-Ingesias, C. *Inorg. Chem.* **2010**, *49*, 4370.

(19) Antanassova, M.; Lachkova, V.; Vassilev, N.; Varabanoa, S.; Dukov, I. *Polyhedron* **2010**, *29*, 655.

(20) Szabo, Z.; Vallet, V.; Grenthe, I. *J. Chem. Soc., Dalton Trans.* **2010**, *39*, 10944.

(21) Quali, N.; Rivera, J.-P.; Chapon, D.; Delange, P.; Piguet, C. *Inorg. Chem.* **2004**, *43*, 1517.

(22) Geraldes, C. F. G. C.; Zhang, S.; Sherry, A. D. *Inorg. Chim. Acta* **2004**, *357*, 381.

(23) Rubini, P.; Ben Nasr, C.; Rodehuser, L.; Delpuech, J.-J. *Magn. Reson. Chem.* **1987**, *25*, 609.

(24) Hooft, R.. *Collect: Data Collection Software*; B.V. Nonius: Delft, The Netherlands, 1998.
(25) Otwinowski, Z.; Minor, W. . In *Macromolecular Crystallography*; Carter, C. W., Jr., Sweet, R. M., Eds.; Academic: Oxford, 1997; Vol. 276, Part A, p 307.
(26) Sheldrick, G. M. *Acta Crystallogr.* **1990**, *A46*, 467.
(27) Sheldrick, G. M. *SHELXL 97, Program for the refinement of crystal structures*; University of Göttingen: Göttingen, Germany, 1997.